Inverse Problems, Design and Optimization Symposium
Rio de Janeiro, Brazil, 2004

AN EFFICIENT PROCEDURE FOR MECHANICAL CHARACTERIZATION OF ORTHOTROPIC MATERIALS

Katia Genovese
Dipartimento di Ingegneria Fisica e dell'Ambiente,
Università degli Studi della Basilicata
Potenza, Italy
genovese@unibas.it

Luciano Lamberti and Carmine Pappalettere
Dipartimento di Ingegneria Meccanica e Gestionale
Politenico di Bari
Bari, Italy.
lamberti@poliba.it, carpa@poliba.it

ABSTRACT

Mechanical characterization of orthotropic materials is a complicated reverse engineering problem. Researchers developed many different methods based on theoretical/numerical formulations or on experimental techniques. In the last few years, integrated techniques that determine elastic constants by comparing experimental results with numerical data have been developed.

The present work discusses a novel hybrid procedure - denoted as ESPI-SA - that includes an optical technique (Electronic Speckle Pattern Interferometry, ESPI) and a numerical optimization technique (Simulated Annealing, SA). ESPI-SA minimizes the difference between the displacement field found experimentally and the displacement field computed numerically (with FEM) by means of an optimization algorithm which finally finds the values of the elastic constants.

In order to check on the feasibility of ESPI-SA, in-plane elastic properties of an orthotropic laminate (8-ply woven fiberglass-epoxy) used as substrate for printed circuit boards have been determined. Specimens were tested in three-point-bending.

Results indicate that ESPI-SA determined accurately the elastic constants of the orthotropic material under investigation. In fact, the residual error between the displacements measured by ESPI and those computed at the end of the simulated annealing identification process was less than 3%. Remarkably, the performance of the ESPI-SA identification procedure was insensitive to the location of the region in which experimental and numerical data are compared.

INTRODUCTION

Experimental identification of mechanical properties of orthotropic materials is a complicated reverse engineering problem entailing several tests each of which requires *ad hoc* setups. Moreover, each test specifically designed for determining a given elastic constant should be run always serially in order to reliably determine the value of that elastic constant on a statistical basis. Finally, because of anisotropy, non-homogeneity and internal defects of the material, different testing procedures may even result in significantly different values of the same elastic constant.

On the other hand, theoretical/analytical models and numerical techniques are certainly much cheaper than experimental techniques in terms of required equipment but they are often based on highly idealized conditions that may be openly in contrast with the real behavior of the material. Moreover, analytical formulations can usually model only a limited set of loading and/or boundary conditions.

From the previous discussion, it appears that an efficient material characterization procedure should determine all the elastic constants by performing a very limited number of experimental tests. *Hybrid techniques* that minimize the difference between experimental and numerical data by means of optimization algorithms where elastic constants are included as design variables certainly satisfy such a requirement and are actually getting more and more common in practical engineering [1-3]. As is clear, a suitable hybrid technique will require: (i) a simple experimental set-up which allows accurate and non-invasive full field measurements; (ii) a robust and reliable optimization procedure able to converge to the target values of elastic properties

regardless of load type, initial guess on elastic constants, boundary conditions, etc.

In view of this, the paper discusses the feasibility of a novel hybrid procedure for characterization of composite materials where *Phase Shifting Electronic Speckle Pattern Interferometry* (PS-ESPI) and *Simulated Annealing* (SA) are combined together in order to minimize the difference between the displacement field gathered experimentally and its counterpart obtained with finite element analysis. The new procedure is indicated as ESPI-SA - the acronym stands for *Electronic Speckle Pattern Interferometry Simulated Annealing* - in the rest of the paper.

Electronic Speckle Pattern Interferometry (ESPI) [4] is a powerful full-field optical technique based on the fact that two beams originated from a coherent light source (i.e., laser) produce an interferometric pattern from which we can recover either correlation fringes and/or phase distribution. Correlation fringes and/or phase distribution are utilized to compute displacements which are proportional to correlation fringe order or to phase difference between loaded and reference (i.e., unloaded) state. As is known, phase-stepping [5] strategies in speckle interferometry (PS-ESPI) are very useful since they allow us to recover directly the phase value yielding at each point of the specimen surface.

Simulated Annealing (SA) [6] is a combinatorial optimization technique where the design variables are perturbed in a random fashion in order to check whether the cost function improves or has a high probability of improving in the next few evaluations. SA is able to find the global optimum with a high probability even for ill-conditioned functions with numerous local minima. In addition, SA does not require gradient information because it does not build approximate models. Therefore, it appears that Simulated Annealing is very suitable for composite material characterization since the identification of elastic constants is certainly a non-smooth problem but with relatively "weak" explicit constraints (i.e., those ensuring positive definiteness of the stiffness matrix).

In ESPI-SA, the difference between numerical and experimental results is expressed in fashion of an error function ψ depending on the material elastic constants to be determined. The ψ function is then minimized by means of the SA based optimizer which finally provides the values of the elastic constants.

Although other material identification techniques [7] process strain values, it should be noticed that strain determination involves numerical differentiation of the displacement field obtained experimentally. However, since the displacement field measured by optical methods will be locally smoothed over a set of pixels close to the location where the value of strain is to be computed, strains might not be correctly estimated. In such a case, the entire identification procedure could fail (see discussion in Ref. 7 for more details).

In addition, strain based material identification procedures lead to write energy balance equations which may require the knowledge of several strain components (for instance, in a 2-D case we need to know ε_x and ε_y under the very limited hypothesis that the cross derivatives $\partial u/\partial y$ and $\partial v/\partial x$ of the x, y displacements do not play any role in the structural response). Determination of in-plane strain components with experimental set-ups based on the Michelson's interferometer principle is a rather well established practice. Hung and Wang [8] built in the middle 1990s a dual beam shearometer for measurement of in-plane strains thus overcoming the limitation of classical shearography which allowed analysts to measure only derivatives of out-of-plane displacements. However, shearographic evaluation of each strain component implies changing the illumination direction. This may be openly in contrast to the requirements on simplicity, repeatability and accuracy of the experimental part included in a hybrid procedure for material identification.

The feasibility of the ESPI-SA procedure has been tested here in the identification of an 8-ply woven reinforced fiberglass-epoxy laminate utilized as substrate for printed circuit boards. Specimens under 3-point-bending have been considered in the experimental tests in order to minimize rigid body motions and thus to prevent speckle pattern de-correlation. The results obtained indicate that ESPI-SA proved itself capable to characterize very well the in-plane behavior of the laminate. In fact, the residual error on computed displacements was less than 3%.

THE ESPI-SA PROCEDURE

Figure 1 shows the flow chart of the ESPI-SA procedure discussed in this paper. The different steps of the procedure are explained in the following.

Experimental determination of the displacement field by means of PS-ESPI

Phase Shifting Electronic Speckle Pattern Interferometry (PS-ESPI) is based on the fact that two beams originated from a coherent light source (laser) produce an interferometric pattern when they hit on a surface. N different interferometric patterns are taken at two different exposures: the reference (i.e., unloaded) and the loaded one. From each set of N acquisition, it is possible to get the distribution of phase $\Phi(x,y)$ at each point of the surface. Finally, displacements are easily computed as they are proportional to the $\Delta\Phi(x,y)$ phase difference between the two different exposures.

Figure 2 shows the experimental set-up based on the Leendertz's interferometer [9] for measurement of in-plane displacements. A 35 mW He-Ne laser (λ=632.8 nm) provides the coherent light source. A closed loop controlled piezoelectric transducer (PZT) is used as phase shifter. The intensity distributions of the combined light beams are recorded by a B/W CCD camera (795 x 596 sensor). The images are then digitized by means of an 8-bit frame grabber. It can be seen from the figure that the laser beam is expanded first, filtered then and collimated finally. In order to preserve coherence, the double illumination is obtained by reflecting a certain fraction of the laser beam onto a mirror (mounted on the PZT device) which is orthogonal to the surface of the specimen. The illumination angle θ made by the laser beams with the direction of observation is 20°. In addition, the aperture of the camera diaphragm is adjusted so to have the best level of illumination and the proper ratio of speckle size to pixel size. Finally, the chosen magnification ratio ensures that the size of the CCD sensor area is about the same as the specimen region investigated.

The displacement field of points on the specimen surface can be determined as follows. The modulated light intensity I(x,y) of a speckle pattern is a harmonic function of the pixel coordinates (x,y). In general, the I(x,y) function has the following analytical form (1):

$$I_r(x,y) = I_o(x,y)\cdot\left[1+\gamma_o(x,y)\cdot\cos\left(\Phi(x,y)+\alpha_r\right)\right]$$

where the r subscript indicates the generic r^{th} acquisition; $I_o(x,y)$ is the average intensity of the light (i.e., a slowly varying background illumination); $\gamma_o(x,y)$ is the fringe contrast; $\Phi(x,y)$ is the value of phase in correspondence of a generic pixel; α_r is the phase-shift angle (between 0 and π) introduced by the difference in optical path Δ_{OP} generated by giving the Δx movement to the PZT device.

In order to get the value of the phase $\Phi(x,y)$ from Eq. (1), one has to determine the unknowns $I_o(x,y)$, $\gamma_o(x,y)$ and $\Phi(x,y)$. Therefore, at least three acquisitions are needed. *Four-phase* technique where shifts are chosen as $\alpha_r = 0^{\circ}, 90^{\circ}, 180^{\circ}, 270^{\circ}$ is widely utilized. Hence, the phase value at the generic pixel (x,y) is:

$$\Phi(x,y) = \arctan\left(\frac{I_4(x,y)-I_2(x,y)}{I_1(x,y)-I_3(x,y)}\right) \qquad (2)$$

where $I_1(x,y)$, $I_2(x,y)$, $I_3(x,y)$ and $I_4(x,y)$ are the light intensity values recorded in the four different acquisitions.

For each pixel, the phase value is determined with Eq. (2) in correspondence of two different exposures: the reference configuration and the loaded configuration. The phase difference $\Delta\Phi(x,y)$ is hence computed for each pixel as:

$$\Delta\Phi(x,y) = \Phi_{loaded}(x,y) - \Phi_{reference}(x,y) \qquad (3)$$

Finally, the displacement u_x in the plane defined by the two illuminating beams (see Figure 2) is:

$$u_x(x,y) = \frac{\Delta\Phi(x,y)}{4\pi}\cdot\frac{\lambda}{\sin\theta} \qquad (4)$$

In-plane displacements were computed in this work by means of an image processing software coded in the Matlab® [10] environment which included spatial filtering and phase unwrapping routines.

Optimization problem

Let u_x^j and $\overline{u_x^j}$ denote the values of in-plane displacement in correspondence of the j^{th} node and pixel respectively determined by means of finite element analysis and by means of PS-ESPI. The barred notation indicates target displacement values since experimental measurements do not require to know the values of elastic constants *a priori*. Conversely, the values of elastic constants must be specified as input to FEM analysis in order to calculate displacements. In view of this, the determination of elastic constants becomes a non-linear optimization problem formulated as follows (5):

$$\begin{cases} \text{Min}\left[\Psi(E_x, E_y, G_{xy}, \nu_{xy}) = \sqrt{\dfrac{1}{Npix}\sum_{j=1}^{Npix}\left(\dfrac{u_x^{\,j} - \overline{u_x^{\,j}}}{\overline{u_x^{\,j}}}\right)^2}\right] \\ E_x > E_y \\ 1 - \nu_{xy}\,(E_y / E_x) > 0 \\ E_x^{\,l} \le E_x \le E_x^{\,u} \\ E_y^{\,l} \le E_y \le E_y^{\,u} \\ G_{xy}^{\,l} \le G_{xy} \le G_{xy}^{\,u} \\ \nu_{xy}^{\,l} \le \nu_{xy} \le \nu_{xy}^{\,u} \end{cases}$$

where the error function Ψ is to be minimized and the elastic constants E_x, E_y, G_{xy} and ν_{xy} are included as optimization variables (the "l" and "u" superscripts denote the lower and upper bounds of elastic constants, respectively). The two additional constrains in expression (5) ensure positive definiteness of the composite stiffness matrix [Q].

The variability range of elastic constants is chosen based on the type of material under investigation. Should this range be not known *a priori*, the identification process will be repeated serially so that each new optimization run starts from the minimum obtained in the previous iteration.

Expression (5) shows that the error function Ψ is built by summing over the difference between the displacements measured by means of PS-ESPI and their counterpart calculated numerically. The difference may be computed at each pixel/node or for a smaller set of points included in the region of interest which is usually located where the speckle set-up ensures enough fringe contrast. Let N_{pix} denote the total number of points (image pixels/FEM nodes) at which the experimental and numerical results are compared. In order to preserve the correspondence between the pixels of the recorded images and the nodes of the FEM model, the FEM model of the specimen is built by setting the element size as a multiple of the pixel size (the limit case obviously occurs when these two sizes are equal).

Since Ψ is certainly a highly non-smooth function, gradient based optimization methods could not work well. In view of this, using Simulated Annealing (SA) in the material identification process is very logical.

Simulated Annealing is a non-gradient optimization technique based on random evaluations of the objective function in such a way that transitions out of a local minimum are possible. The design variables are perturbed in a random fashion in order to check whether the cost function ψ improves or has a high probability of improving in the next few evaluations. Candidate designs are immediately accepted if they result in improvement in cost ($\Delta\Psi<0$). Conversely ($\Delta\Psi>0$), the SA algorithm accepts/rejects intermediate designs based on a probability function which depends on a parameter called "temperature": as the temperature decreases, the probability of improving the cost further gets lower. It is apparent that SA is a global optimization algorithm because random generation of candidate designs allows us to explore larger fraction of design space than in approximate optimization where sensitivity analysis and search of candidate designs are performed only in the neighbourhood of the design point about which the problem is approximated.

The pseudo code of the SA based optimizer is now provided (also see the flow chart shown in Figure 1).

1. Start the optimization process. Store the elastic constants in the design vector $\mathbf{X}(x_1, x_2, x_3, x_4)$ where x_1, x_2, x_3 and x_4, respectively, are the E_x, E_y, G_{xy} and ν_{xy} constants. Set the K value for the counter of cooling cycle as 1.
2. Choose an initial design for which the value of the Ψ function is very high. Store the initial design in the $\mathbf{X_{OPT}}$ vector. Denote the corresponding value of the error function as Ψ_{OPT}.
3. Set the initial temperature as T_o=1000 and choose the reduction factor β. In general, it is suggested $0.9 \le \beta \le 0.99$. Here, we used an average value: β=0.95.
4. Execute a cooling cycle. Perturb randomly each design variable x_i (i=1,…,4) as follows (6):

$$N_{RND}<0 \Rightarrow x_i = x_{OPT,i} + (x_{OPT,i} - x_i^{\,l})\, N_{RND}\,(T_K / T_o)$$
$$N_{RND}>0 \Rightarrow x_i = x_{OPT,i} + (x_i^{\,u} - x_{OPT,i})\, N_{RND}\,(T_K / T_o)$$

where N_{RND} is a random number chosen in the interval (–1, 1). The T_K/T_o ratio is initially set equal to 1 and is shrunk as the optimization progresses.

Perturb one design variable at a time and generate hence four new design vectors $\mathbf{X}_i$.

5. Evaluate the cost function at each one of the designs randomly generated in Step 4. Let Ψ_i denote the value of the error function in correspondence of the design $\mathbf{X}_i$ generated by changing only the i^{th} variable. Compare each Ψ_i to Ψ_{OPT} and compute $\Delta\Psi_i = \Psi_i - \Psi_{OPT}$.
   - If it holds $\Delta\Psi_i<0$, accept the design $\mathbf{X}_i$ as the new optimum $\mathbf{X_{OPT}}$. Set $\Psi_{OPT} = \Psi_i$.
   - If it holds $\Delta\Psi_i>0$, generate a random number ρ in the interval (0,1). Based on the Metropolis criterion [6], accept a design $\mathbf{X}_i$ if it occurs $P(\Delta\Psi_i)=e^{\frac{-\Delta\Psi_i}{k_B T_K}}>\rho$ (k_B is the Boltzmann's parameter) while reject the design $\mathbf{X}_i$ if it occurs $P(\Delta\Psi_i)<\rho$. The rationale behind this criterion is that any perturbation of design which does not yield immediate improvement in cost function is however retained if the corresponding design point helps to bypass a local minimum increasing, thus, the probability of reaching the global optimum.

   Increase the number N_{acc} of accepted designs in a secondary cycle each time $\Delta\Psi_i<0$ or $P(\Delta\Psi_i)>\rho$.
6. Stop optimization process and go to Step 9 if it occurs $N_{acc}=0$. If it occurs $N_{acc}>0$ in the K^{th} cooling cycle, store Ψ_{OPT} as $\Psi_{OPT,K}$.
7. If K>3 check for convergence according to the following criterion:

$$\text{Max}\left[\frac{|W_{OPT,K}-W_{OPT,K-1}|}{W_{OPT,K}};\ \frac{|W_{OPT,K-1}-W_{OPT,K-2}|}{W_{OPT,K-1}};\ \frac{|W_{OPT,K-1}-W_{OPT,K-2}|}{W_{OPT,K-1}};\ \frac{|W_{OPT,K-2}-W_{OPT,K-3}|}{W_{OPT,K-2}}\right] \qquad (7)$$

where $W_{OPT,K}$ denotes the best record found in the K^{th} cooling cycle. The ε_{CONV} parameter is set to 10^{-5}. If the convergence criterion is satisfied go to Step 9.

8. If K<3 or the convergence criterion (7) is not satisfied:
   - reset the K counter as K=K+1, $N_{acc}=0$;
   - reduce temperature in fashion of $T_K = \beta T_{K-1}$;
   - repeat from Step 4 onward.
9. End the optimization process.

RESULTS AND DISCUSSION

The ESPI-SA procedure for mechanical characterization of orthotropic materials described in this work was tested on an 8-ply woven reinforced fiberglass-epoxy composite utilized as substrate for printed circuit boards. Standard mechanical tests previously carried out on the material provided the following elastic properties: E_x=25 GPa; E_y=22 GPa; G_{xy}=5 GPa; ν_{xy}=0.28.

Figure 3 shows the composite laminate to be characterized. A 46 mm long, 13 mm tall and 1.2 mm thick specimen was cut from a slice of material. The specimen, subjected to 3-point-bending, was mounted on two supports spaced by 30 mm. The 140 N vertical force which generated the load state was applied to the specimen by a rounded tip mounted on a sledge moved by a micrometric screw. Such a value of load preserved correlation of speckle patterns and ensured a rather high density of phase fringes. Indeed, the 3-point-bending load was chosen in this study because it minimizes rigid body motions (RBMs) of the specimen during the loading phase. This is very useful since RBMs may invalidate measurements carried out with PS-ESPI as they cause speckle pattern de-correlation.

The phase distribution obtained by means of PS-ESPI (with the Four-frame technique) is shown in Figure 4. It can be seen that the phase fringes reproduced the u_x displacement field in fashion of a saw-tooth pattern. The loaded zone and the simply-supported zone are approximately indicated in the figure.

Figure 4 also shows the FEM model used in the SA based optimization process along with the locations at which numerical and experimental data were compared. The commercial finite element code ANSYS® [11] was utilized to perform structural analyses in the identification procedure. The specimen was modeled with PLANE42 elements each of which included four

nodes and two degrees of freedom per node. Since the specimen thickness is very small compared to the distance between supports, the plane-stress state is assumed in the specimen. Because of symmetry about the vertical axis and limitations in size of the optics used in the experiments, the region of interest considered along the x-direction was about 18 mm long.

Since the ESPI set-up used in the experiments allowed to measure horizontal displacements (see Figure 2), the Ψ error function was built by comparing the numerical (FEM) and experimental (PS-ESPI) values of u_x displacements at the three locations indicated in Figure 4. The "5 mm" and "10 mm" locations are uniformly spaced with respect to the axis of symmetry of the specimen and the location of the simple-support while the "16.5 mm" station is very close to the support. The Ψ error function was minimized in all those three cases. Finally, an additional optimization run (indicated as "ALL" in the rest of the paper) included all the nodes/pixels considered in the other three runs.

Table 1 presents the results obtained for the material identification procedure. Different initial guesses on material properties were made in order to introduce more uncertainty in the optimization. It appears from the table that ESPI-SA was insensitive to the initial guess on elastic constants and to the location of the node sets chosen as basis of comparison in the material identification process. ESPI-SA was able to recover the very large initial percentage errors.

Remarkably, the values of elastic constants determined by means of ESPI-SA were very close to the target values. Therefore, the ESPI-SA procedure achieved an acceptable final accuracy since the largest error on horizontal displacements was less than 3%. This residual error was certainly caused by uncertainty factors such as electronic noise mixed with interferometric patterns, overall efficiency of filtering process, local de-correlation of speckle patterns, etc.

Figure 5 shows the percentage error on the u_x displacement computed at each node/pixel of the different control stations ("5 mm", "10 mm", "16.5 mm", "ALL") when the values of elastic constants determined by the SA based optimizer were given as input to the FEM code. It can be seen that the maximum error occurred near the middle of the specimen height: that is, where the bending neutral axis is approximately located. This happened because the horizontal displacements are much smaller near the neutral axis than at the bottom and the top of the specimen and hence the optimizer is more sensitive to sudden changes in u_x displacement sign which may result in local peaks of the Ψ error function. Such a behaviour was seen for all control stations. However, the simple-support located near the "16.5 mm" station resulted in increasing the standard deviation value of the error distribution.

CONCLUSIONS

This paper described a novel hybrid procedure for mechanical characterization of orthotropic materials. The procedure – named as ESPI-SA (Electronic Speckle Pattern Interferometry - Simulated Annealing) – combined a powerful optical technique (PS-ESPI) for full-field in-plane displacement measurements and a non-gradient optimizer (SA) particularly suitable for highly non-linear and non-smooth problems. The rationale behind ESPI-SA is to minimize the Ψ difference between the displacements computed by means of finite element analyses and their counterpart measured experimentally. Therefore, the Ψ difference was expressed here in fashion of an error function depending on the elastic constants of the material to be characterized. In summary, the reverse engineering problem of material characterization became an optimization problem where the goal is to minimize the Ψ function and the elastic constants are included as design variables.

An 8-ply woven reinforced fiberglass-epoxy laminate used as substrate for printed circuit boards was characterized by means of the ESPI-SA procedure described in this paper. A 46 mm long, 13 mm tall and 1.2 mm thick specimen was cut from a slice of material. The specimen was subjected to 3-point-bending in order to preserve correlation of speckle patterns. Horizontal displacements were measured with a set-up based on the Leendertz's double illumination interferometer. Different sets of nodes were chosen at three locations in order to build the Ψ error function. An additional optimization run included all the nodes simultaneously. The Ψ difference was then minimized by means of the SA based optimizer.

The results obtained in this study indicate that the ESPI-SA procedure was capable to accurately characterize the behavior of the 8-ply woven composite laminate. In fact, the residual error

between the displacements measured by means of PS-ESPI and those computed by means of finite element analysis at the end of the identification process was less than 3%. Most of this error was probably due to factors inherent to ESPI (electronic noise, filtering efficiency, etc.).
However, even though the proposed approach to orthotropic material characterization proved itself to be feasible and the results presented in this paper were encouraging, the present authors point out that other experiments should be carried out in order to certify ESPI-SA as a "black-box" procedure for in-plane mechanical characterization of orthotropic materials.

REFERENCES

1. H. Sol, H. Hua, J. De Visscher, J. Vantomme and W.P. De Wilde, A mixed numerical/experimental technique for the nondestructive identification of the stiffness properties of fibre reinforced composite materials, *NDT-E Int*., **30**, 85-91 (1997)

2. S. Hwang and C. Chang, Determination of elastic constants of materials by vibration testing, *Compos. Struct.*, **49,** 183-190 (2000).

3. R. Rikards, A. Chate and G. Gailis, Identification of elastic properties of laminates based on experiment design, *Int. J. Solids Struct.*, **38**, 5097-5115 (2001).

4. G.L. Cloud, *Optical methods of Engineering Analysis*, Cambridge University Press, New York (USA), 1998.

5. K. Creath, Phase-shifting Speckle Interferometry, *Appl. Opt.*, **24**, 3053-3058 (1985).

6. S.S. Rao , *Engineering optimization*, Wiley Interscience, New York (USA), 1996.

7. M. Grediac, F. Pierron and Y. Surrel, Novel procedure for complete in-plane composite characterization using a single T-shaped specimen, *Exp. Mech.*, **39,** 142-149 (1999).

8. Y.Y. Hung and J.Q. Wang, Dual-beam shift shearography for measurement of in-plane strains, *Opt. Las. Eng*., **24,** 403-413 (1996).

9. J.A. Leendertz, Interferometric displacement measurement on scattering surface utilizing speckle effect, *Journal of Physics E: Sci. Instrum*, **3,** 214-218 (1970).

10. MathWorks Matlab® Version 6.1, http://www.mathworks.com.

11. The ANSYS® 7.0 User's Manual, Swanson Analysis System Inc., 2003.

Table 1. Sensitivity of ESPI-SA performance to experimental data

Location where data are compared	**x = 5 mm**	**X = 10 mm**	**x = 16.5 mm**	**All locations**
Initial values of elastic constants*	$E_x = 5000$ $E_y = 3000$ $G_{xy} = 2000$ $\nu_{xy} = 0.1$	$E_x = 10000$ $E_y = 8000$ $G_{xy} = 2000$ $\nu_{xy} = 0.4$	$E_x = 30000$ $E_y = 10000$ $G_{xy} = 8000$ $\nu_{xy} = 0.01$	$E_x = 3000$ $E_y = 2000$ $G_{xy} = 1000$ $\nu_{xy} = 0.01$
Initial % error on u_x				
Average	140.1 %	146.6 %	37.6 %	281 %
Maximum	197.4 %	226.2 %	148.4 %	870 %
Calculated values of elastic constants	$E_x = 25016$ $E_y = 22049$ $G_{xy} = 5002$ $\nu_{xy} = 0.281$	$E_x = 25048$ $E_y = 21989$ $G_{xy} = 5035$ $\nu_{xy} = 0.279$	$E_x = 25031$ $E_y = 21963$ $G_{xy} = 4969$ $\nu_{xy} = 0.279$	$E_x = 25043$ $E_y = 22034$ $G_{xy} = 5000$ $\nu_{xy} = 0.279$
Final % error on u_x				
Average	1.351 %	1.469 %	1.118 %	2.033 %
Maximum	2.711 %	2.481 %	2.180 %	2.775 %

Target values: $E_x = 25$ GPa ; $E_y = 22$ GPa; $G_{xy} = 5$ GPa; $\nu_{xy} = 0.28$

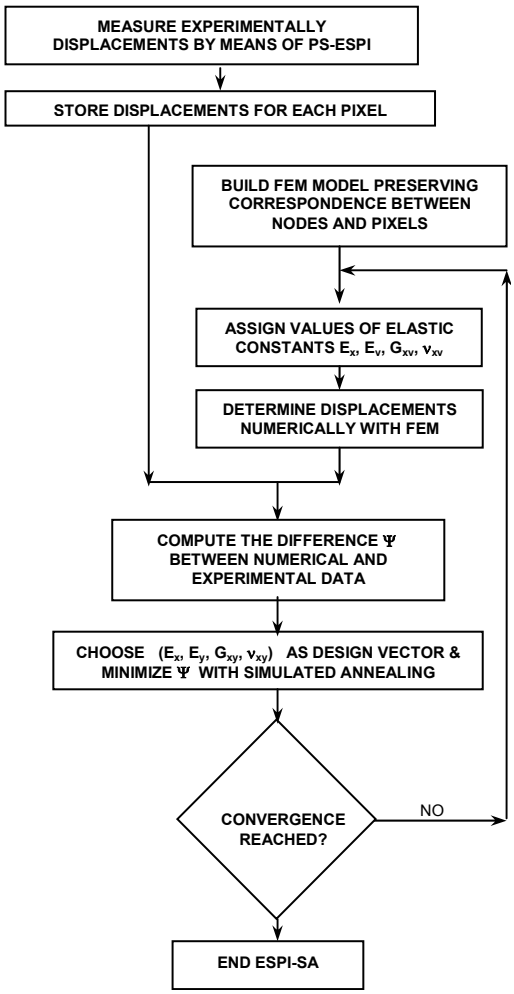

Figure 1. Flow-chart of ESPI-SA

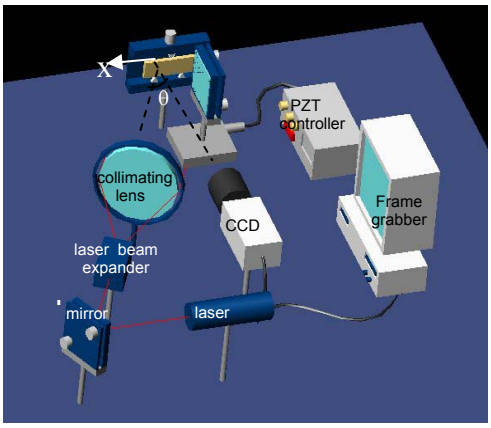

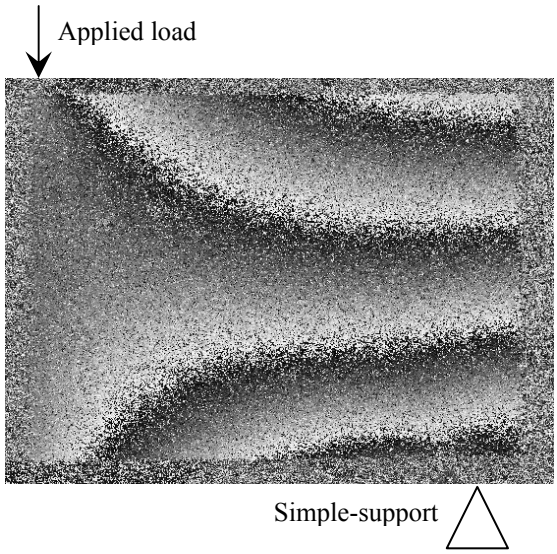

Figure 2. Schematic of the experimental set-up

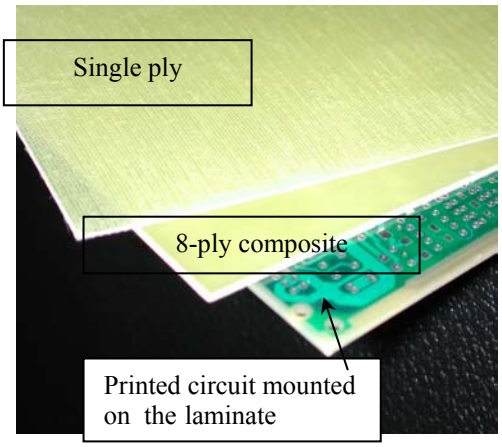

Figure 3. Reinforced fiberglass-epoxy laminate characterized with ESPI-SA

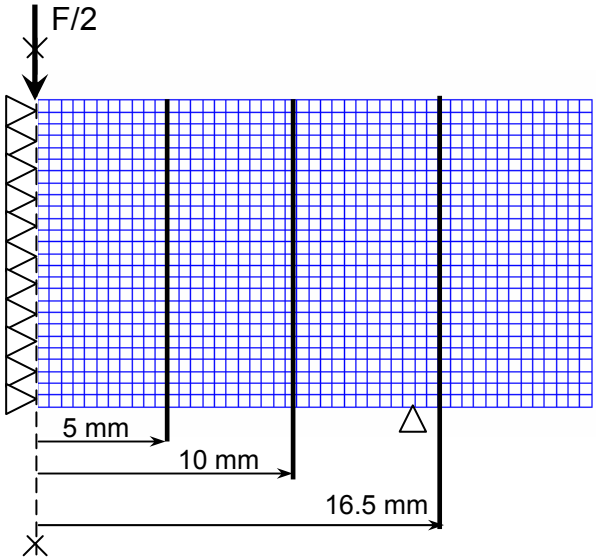

Figure 4. Phase map obtained with PS-ESPI. FEM model used in the identification procedure

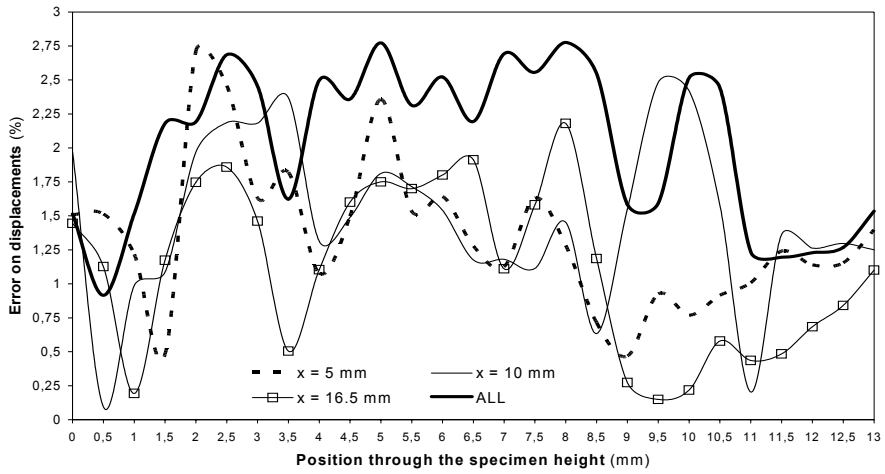

Figure 5. Residual percentage error on u_x displacements after the identification process